High pressure gas flow, storage, and displacement in fractured rock - Experimental setup development and application

Hadi Mosleh, M.; Turner, M.; Sedighi, M.; Vardon, P. J.

DOI
10.1063/1.4973963

Publication date
2017

Document Version
Final published version

Published in
Review of Scientific Instruments

Review of Scientific Instruments

High pressure gas flow, storage, and displacement in fractured rock—Experimental setup development and application

Cite as: Rev. Sci. Instrum. **88**, 015108 (2017); https://doi.org/10.1063/1.4973963
Submitted: 14 June 2016 . Accepted: 22 December 2016 . Published Online: 19 January 2017

M. Hadi Mosleh, M. Turner, M. Sedighi, and P. J. Vardon



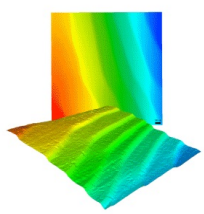
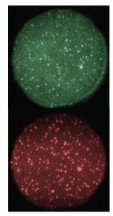

AIP Publishing

High pressure gas flow, storage, and displacement in fractured rock—Experimental setup development and application

M. Hadi Mosleh,[1,2,a)] M. Turner,[1,3] M. Sedighi,[1,4] and P. J. Vardon[1,5]
[1]*Geoenvironmental Research Centre, School of Engineering, Cardiff University, The Queen's Buildings, Newport Road, Cardiff CF24 3AA, United Kingdom*
[2]*Royal School of Mines, Department of Earth Sciences and Engineering, Imperial College London, London SW7 2AZ, United Kingdom*
[3]*IHS Global Limited, Enterprise House, Cirencester Road, Tetbury GL8 8RX, United Kingdom*
[4]*School of Mechanical, Aerospace and Civil Engineering, The University of Manchester, Sackville Street, Manchester M13 9PL, United Kingdom*
[5]*Section of Geo-Engineering, Faculty of Civil Engineering and Geosciences, Delft University of Technology, 2600 GA Delft, The Netherlands*

(Received 14 June 2016; accepted 22 December 2016; published online 19 January 2017)

This paper presents the design, development, and application of a laboratory setup for the experimental investigations of gas flow and reactions in a fractured rock. The laboratory facility comprises (i) a high pressure manometric sorption apparatus, where equilibrium and kinetic phenomena of adsorption and desorption can be examined, (ii) a high pressure triaxial core flooding system where the chemical reactive transport properties or processes can be explored, and (iii) an ancillary system including pure and mixed gas supply and analysis units. Underground conditions, in terms of pore pressure, confining pressure, and temperature, can be replicated using the triaxial core flooding system developed for depths up to 2 km. Core flooding experiments can be conducted under a range of gas injection pressures up to 20 MPa and temperatures up to 338 K. Details of the design considerations and the specification for the critical measuring instruments are described. The newly developed laboratory facility has been applied to study the adsorption of N_2, CH_4, and CO_2 relevant to applications in carbon sequestration in coal and enhanced coalbed methane recovery. Under a wide range of pressures, the flow of helium in a core sample was studied and the evolution of absolute permeability at different effective stress conditions has been investigated. A comprehensive set of high resolution data has been produced on anthracite coal samples from the South Wales coalfield, using the developed apparatus. The results of the applications provide improved insight into the high pressure flow and reaction of various gas species in the coal samples from the South Wales coalfield. *Published by AIP Publishing.* [http://dx.doi.org/10.1063/1.4973963]

I. INTRODUCTION

Complex physical and chemical phenomena can be involved in gas flow in a fractured rock. An increase in deep sub-surface energy applications such as unconventional gas exploitation and geological carbon sequestration has highlighted the importance of having a comprehensive and detailed understanding of the processes that can occur during gas injection and recovery in deep geological strata. It is therefore critical to produce high resolution and comprehensive experimental datasets that can be utilised to reliably predict the design of industrial applications.[1]

Gas transport in coal includes the flow through the naturally fractured porous network (cleats), diffusion into the coal matrix, and storage/displacement within the micropores in an adsorbed state.[2] Complex physical, chemical, and mechanical processes are involved in the reactive transport process of gases in coal and especially in the case of carbon dioxide.[3] Despite the extensive effort to explore the complex and coupled phenomena involved, there is a lack of understanding of the processes that can occur when carbon dioxide is injected into the coal seams. The challenge is mainly related to the fact that transport processes are highly related to the chemical and physical changes to the coal structure during adsorption and desorption processes.[3]

A wide range of experimental methods have been used to study the adsorption and desorption isotherms of gases in coal. The methods include (i) gravimetric,[4–6] (ii) volumetric/manometric,[7–10] (iii) carrier gas and calorimetric techniques,[11] (iv) nuclear resonance,[12] and chromatographic analysis.[13] Among the methods mentioned, the most frequently used are the volumetric or manometric methods. Most of the commercially available sorption apparatuses however are only applicable for small size samples (usually volume of less than 1 ml), limiting the investigation of large size samples or intact rocks.

A number of laboratory developments and investigations have been reported on the transport of gases in coal through core flooding experiments. The apparatus and approaches reported in the literature include (1) a True Triaxial Stress Coal Parameter (TTSCP) facility to measure the coal permeability to CO_2 using a quasi-steady flow method;[14,15] (2) a high-pressure core flooding setup comprising a pressure cell, a

a)Author to whom correspondence should be addressed. Electronic mail: m.hadi-mosleh@imperial.ac.uk

syringe pump, and a micro gas chromatographer;[16–19] and (3) a high pressure triaxial apparatus capable of measuring the flow rate and deformation of the core samples.[20–23] Among the mentioned methods, the triaxial flooding approach has received more attention compared to other methods due to its capability to replicate the *in situ* stress conditions at different depths. Using a triaxial cell, the permeability of porous rock under underground stress conditions can be measured using a steady-state method, an unsteady-state method, or a transient approach.[24,22]

Based on published works it can be highlighted that the majority of the experimental apparatuses have been specifically developed to investigate certain areas, e.g., gas sorption in coal, gas transport in coal, or swelling/shrinkage of coal.

This paper presents the developments of a laboratory facility which offers a more detailed and comprehensive set of experimental tools for the investigations of coal-gas interactions. The features of the facilities developed enable a simultaneous run of the experiments using both units, i.e., the gas sorption apparatus and the triaxial core flooding system. This is considered to be an important advantage due to the long-term nature of the experiments. In addition, the data produced from both units provide a series of experimental results that can be used in the modeling of processes such as gas storage and recovery in coal.

Details of the laboratory facility designed and commissioned to study the interactions of high pressure gases with a fractured rock are presented. The design considerations and the specification for the critical measuring instruments are described. The newly developed laboratory facility has been applied to study aspects related to the coal interactions with N_2, CH_4, and CO_2 relevant to carbon sequestration in coal and enhanced coalbed methane (CO_2-ECBM) recovery. Under a wide range of pressures, the adsorption/desorption properties and the reactive flow and displacement of the gases in coal can be studied using the developed laboratory facilities. The experimental procedures and measurement methods are described. The results of adsorption tests on powdered coal samples as well as the permeability variations of core samples at different injection and confining pressures are also presented.

II. DESIGN AND DEVELOPMENT OF THE LABORATORY FACILITY

The experimental facility consists of (i) a high pressure manometric sorption apparatus by which the equilibrium and kinetic phenomena of adsorption and desorption can be examined, (ii) a high pressure triaxial core flooding system by which the reactive transport properties or processes can be obtained and explored, and (iii) the ancillary system including pure and mixed gas supply and analysis units. A schematic diagram of the developed laboratory facility is presented in Figure 1.

A. The manometric sorption apparatus

The manometric method has been adopted in this work for measuring the excess adsorption/desorption isotherms of different gas species. Manometric apparatus comprises two pressure vessels, the reference cell and the sample cell. Both cells are connected via a valve and the gas pressure inside each cell is monitored by pressure transducers. The temperature of the system is kept constant using a water bath.

In order to obtain a wide range of equilibrium pressures (to be able to produce data for high pressure-high adsorption systems), the manometric apparatus was designed considering the critical parameters that directly control the range of equilibrium pressure in a manometric apparatus as identified by Gensterblum *et al.*[25] and Mohammad *et al.*[26] The parameters considered are (i) the maximum gas injection pressure, (ii) the volumetric ratio of the sample cell to the reference cell (V_{SC}/V_{RC}), and (iii) the void volume, i.e., the volume unoccupied by the sample.

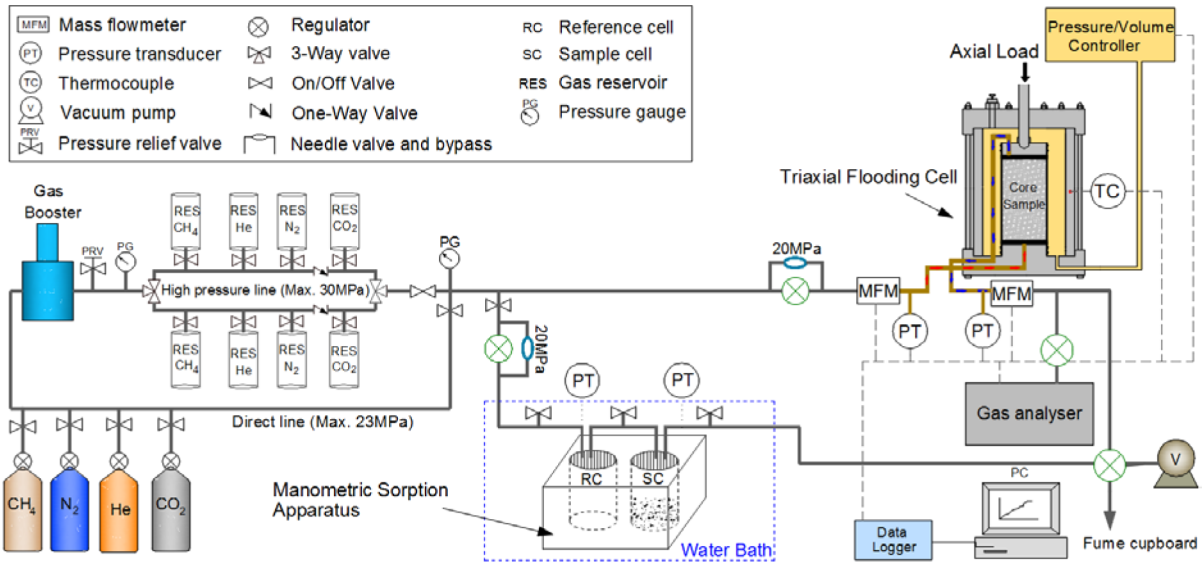

FIG. 1. A schematic diagram of the developed laboratory facility.

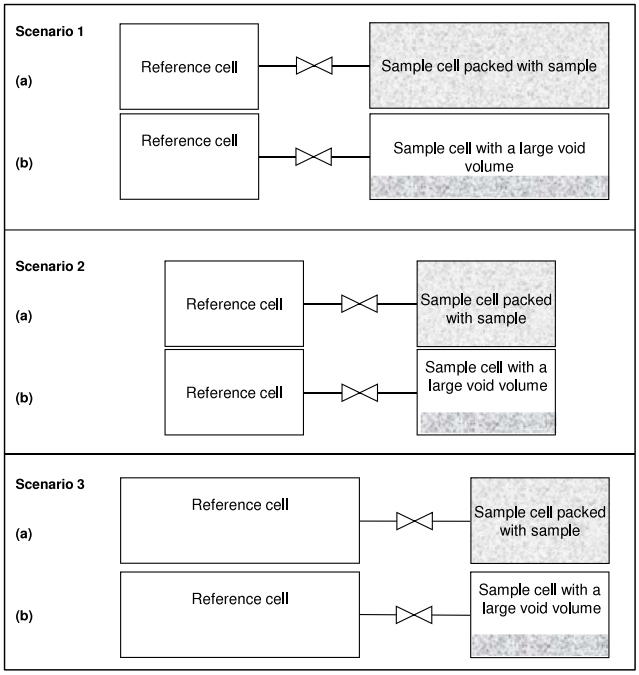

FIG. 2. Schematic diagram of the defined scenarios for the design of the manometric cell.

Considering the application of this apparatus for carbon storage and methane recovery in South Wales coalfield, the range of gas pressures in this area is not expected to exceed 20 MPa, and therefore the adsorption cell was designed for a maximum pressure of 20 MPa.

In order to optimise the volumetric ratio of the sample cell to the reference cell (V_{SC}/V_{RC}), a number of possible arrangements for the adsorption cell were considered that include (V_{SC}/V_{RC}) to be 2, 1, and 0.5 (Figure 2). Each case was also divided into two subdivisions. For subdivisions (a), the sample cell was assumed to be packed with a powder sample in order to minimise the void volume. In the case of subdivisions (b), the sample cell was assumed to be partially filled with the sample resulting in a large void volume that remained in the cell.

According to Gensterblum *et al.*,[25] a (V_{SC}/V_{RC}) ratio between 1 and 10 can result in lower errors but also in smaller pressure steps. Therefore, more pressure steps are required to reach the final pressure. Mohammad *et al.*[26] defined a (V_{SC}/V_{RC}) ratio of 2 as the upper limit due to the constraint on the maximum injection pressure in practice. In addition and in order to obtain higher equilibrium pressures and minimise the experimental uncertainties, the void volume in the adsorption cell should be reduced by using as much sample as possible in the sample cell.[26]

Based on the mass conservation law and ideal gas law, the amount of gas in a manometric system can be estimated as[27]

$$\frac{P_1V_1}{Z_1RT} = \frac{P_2V_2}{Z_2RT} = \frac{P_3V_3}{Z_3RT} + n_{ads}^{ex}, \quad (1)$$

where P_1, P_2, and P_3 are the gas pressures (Pa) in the reference cell initially, after connecting the cells and at equilibrium state, respectively. Z_1, Z_2, and Z_3 are the corresponding gas compressibility factors to P_1, P_2, and P_3, respectively. R is the universal gas constant (J/mol K) and T is gas temperature (K). V_1, V_2, and V_3 are the free gas volumes at each stage. In a real experiment, the parameters P_1, P_2, and P_3 are the known values, i.e., are obtained from direct measurements. Therefore, Z_1 to Z_3 can be estimated using equation of state (EoS). The amount of excess gas adsorption/desorption is then calculated based on the estimated values. At the stage of the design, however, the experimental parameters (gas pressure variations) are not available. Therefore, a back-calculation analysis was carried out to predict the gas pressure variations during gas adsorption process. In these analyses, parameters and material properties associated with CO_2 and coal were used due to their relevance to the application of this study:

- Gas injection pressure was considered to be between 1 and 20 MPa.
- Two temperature values were considered to be 313 K and 328 K.
- Gas compressibility factor was estimated based on Peng-Robinson Equation of State (PR-EoS).[28]
- Two sizes of cell volumes were considered for the reference cell and sample cell to be 1×10^{-4} m^3 or 5×10^{-5} m^3. The values of the sample volume and void volume considered are presented in Table I.
- The amount of excess adsorption was estimated based on absolute adsorption parameters (Langmuir coefficients and adsorbed-phase density) for the Selar Cornish coal, suggested in the literature.[25]

After performing the analyses, the results of gas pressure variations during gas injection and adsorption were plotted for each scenario. Details of the analyses and plots of gas pressure variations can be found in the work of Hadi Mosleh.[29] Table II presents a summary of the results and comparison between different scenarios with regards to the design considerations, i.e., providing more accurate pressure resolutions and maximum equilibrium pressures. Based on

TABLE I. The values of the sample volume and void volume considered in the development of scenarios.

Scenario		V_{SC}/V_{RC} (−)	V_{RC} (m^3)	V_{SC} (m^3)	m_s (kg)	V_s (m^3)	V_v (V_{SC}-V_s) (m^3)	V_v/V_s (−)
1	a	2	5.0×10^{-5}	1.0×10^{-4}	0.140	9.3×10^{-5}	6.7×10^{-6}	0.1
	b	2	5.0×10^{-5}	1.0×10^{-4}	0.050	3.3×10^{-5}	6.7×10^{-5}	2.0
2	a	0.5	1.0×10^{-4}	5.0×10^{-5}	0.065	4.3×10^{-5}	6.7×10^{-6}	0.2
	b	0.5	1.0×10^{-4}	5.0×10^{-5}	0.020	1.3×10^{-5}	3.7×10^{-5}	2.8
3	a	1	5.0×10^{-5}	5.0×10^{-5}	0.060	4.0×10^{-5}	1.0×10^{-5}	0.3
	b	1	5.0×10^{-5}	5.0×10^{-5}	0.010	6.7×10^{-6}	4.3×10^{-5}	6.5

TABLE II. Comparison of the results of different scenarios after accounting for the design considerations. (√): The results of analyses for the defined scenario are in agreement with the design considerations; (×): the results do not fulfill the design considerations.

Scenarios		Design considerations			
		Minimum required pressure resolution (MPa)		Maximum equilibrium pressure (MPa)	
1	a	0.033	(√)	13.5	(√)
	b	0.001	(×)	9.5	(×)
2	a	0.006	(×)	16	(√)
	b	0.002	(×)	13	(√)
3	a	0.017	(√)	14	(√)
	b	0.002	(×)	11	(×)

Table II, scenario (2a) was found to be the most appropriate and optimised arrangement with regards to the critical parameters discussed above. Another advantage of this arrangement is that less pressure steps are required to reach the final equilibrium pressure (due to its smaller sample cell) and therefore, the equilibrium state can be achieved faster compared to other scenarios.[29]

The constructed and commissioned manometric sorption apparatus comprises a double-ended twin cavity block of stainless steel (SS-316) with caps (Figures 3 and 4). The cavity on the left-hand side is considered as the reference cell and the cavity on the right-hand side is considered as the sample cell. The cells have a volume of 150 cm^3 each, excluding a 0.24 cm^3 dead volume of the tubes and the valves. Nitrile and Viton O-rings have been used as a seal between the cell body and the cap. Two in-line pressure transducers with 2 kPa resolution and 0.15% of accuracy and three stainless steel needle valves were employed for the adsorption cell (Figure 4). Swagelok

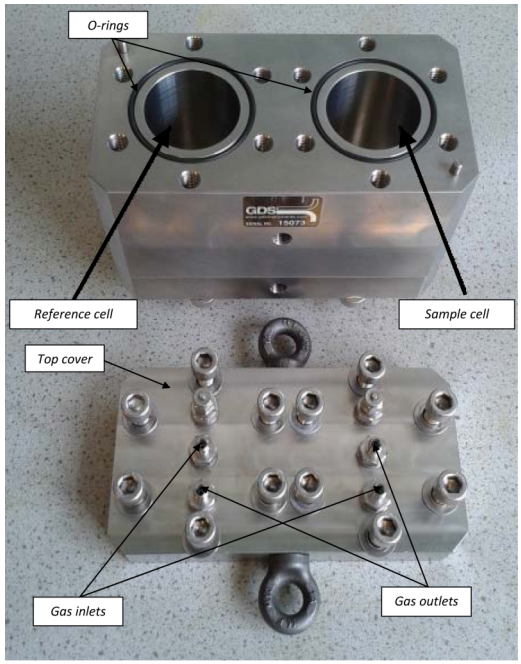

FIG. 3. Adsorption cell including a reference cell and a sample cell.

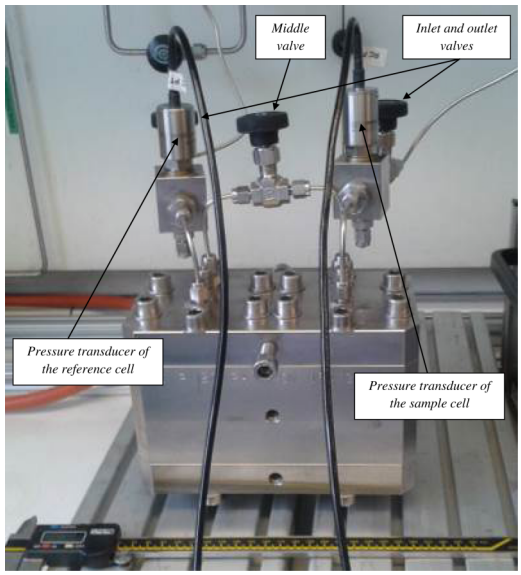

FIG. 4. Arrangement of the pressure transducers and three needle valves.

stainless steel flexible tubes (SS-316 with O/D of 1/8 in.) were used to connect the valves and pressure transducers to the cells. The flexible tubes were pressure certified for up to 8500 psi (58 MPa) gas pressure and therefore it was expected that their internal volume does not change with pressure. The dead volumes including the internal volumes of stainless steel tubes, valves, and transducers were measured and taken into account during void volume measurements using the helium pycnometry method. An in-house built stainless steel water tank ($0.3 \times 0.3 \times 0.3$ m) and a Thermo Haake temperature controller with an accuracy of ±0.01 K have been used to provide a constant temperature for the adsorption cell and its components throughout testing.

B. The triaxial core flooding system

In order to investigate the flow processes in a rock material, triaxial testing has been utilised more frequently especially for measurements at high pressure conditions.[23,20] Steady-state core flooding experiments are commonly conducted on a core sample under confined conditions and by applying gas pressure to one end and measuring the flow rate and pressure differential under the steady-state conditions.[24] For the measurement of gas flow rates during core flooding experiments, a flow meter with high accuracy, e.g., 0.5% of Full Range Output (FRO), is required to be incorporated into the flow measurement system. The flow meters were expected to be capable of measuring the lowest and highest possible flow rates that occur during the experiments. The range of lowest and highest possible gas flow rates were estimated based on Darcy's equation for gases,[30]

$$Q_0 = \frac{k_g A(P_{up}^2 - P_{down}^2)}{2\mu_g L P_0}, \tag{2}$$

where Q_0 is the volumetric rate of flow at reference pressure (m^3/s), k_g is the gas permeability coefficient (m^2), μ_g is the gas viscosity (Pa s) calculated from the relationship provided

TABLE III. Parameters considered for estimating the range of gas flow rates to be expected in core flooding experiments.

	Scenario			
Parameter	1	2	3	4
Sample diameter and length (m)	D:0.025; L:0.05	D:0.025; L:0.05	D:0.01; L:0.02	D:0.01; L:0.02
Permeability (m^2)	1×10^{-17}	3×10^{-15}	1×10^{-17}	3×10^{-15}
Maximum upstream pressure (MPa)	20	20	20	20
Downstream pressure (MPa)	0.1	0.1	0.1	0.1
Viscosity of CO_2 at 313 K (Pa.s)	1.57×10^{-5}	1.57×10^{-5}	1.57×10^{-5}	1.57×10^{-5}
Viscosity of CO_2 at 328 K (Pa.s)	1.64×10^{-5}	1.64×10^{-5}	1.64×10^{-5}	1.64×10^{-5}
Maximum expected gas flow rate (m^3/s)	13×10^{-6}	4×10^{-3}	199×10^{-6}	60×10^{-3}

by Smits and Dussauge,[31] L is the sample length (m), P_0 is the reference pressure (Pa), A is the cross-sectional area of the sample (m^2), P_{up} is the upstream gas pressure (Pa), and P_{down} is the downstream gas pressure (Pa).

A number of scenarios were defined based on a range of sample sizes, permeability values, gas pressures, and temperatures (Table III). The result of gas flow rates calculated for each scenario, using Equation (2), showed that a broad range of gas flow rates can be expected during the experimental measurements, i.e., 13×10^{-6} to 60×10^{-3} m^3/s. On the other hand, most of the commercially available flow meters are limited to a certain range of gas flow rates. For instance, some flow meters are designed for low flow rates up to 1.7×10^{-6} m^3/s (100 ml/min) and some are designed to measure high flow rates up to 17×10^{-6} m^3/s (1 l/min). Eventually, it was decided to adopt a mass flow meter capable of measuring high flow rates up to 17×10^{-6} m^3/s (1 l/min). Instead, for the experiments with high permeable samples such as highly fractured coals or sandstones, higher injection pressures can be avoided so that the gas flow rate would not exceed the upper limit of the flow meter. Alternatively, a back pressure regulator can be used to adjust the gas flow rate before passing through the mass flow meter. These flow meters are capable of working under both subcritical and supercritical conditions with pressures up to 20 MPa and accuracy of 0.5% full range output.

The constructed and commissioned triaxial cell includes a base pedestal, a top-cap, an internal submersible load cell, and local strain transducers. The core sample sits within a silicon sleeve (Figure 5) and the test gas passes through a porous plate at the bottom of the sample, then it leaves the cell through a similar arrangement at the top after having passed through the test core.

Two axial and one radial high pressure Linear Variable Differential Transformer (LVDT) local strain transducers from GDS Instruments are attached to the sleeve (Figure 5) to measure the volumetric deformation of the sample with an accuracy of 0.1% of ±5 mm full range output. The LVDT transducers have a maximum operating pressure of 200 MPa in non-conductive oil only. In addition, a ±0.025 m displacement transducer with an accuracy of 0.25% has been used to measure the axial displacement of the sample due to increase or decrease in axial loads applied by the load frame. The transducers are capable of working at temperature up to 333 K (60 °C).

1. Pressure control system

The range of gas pore pressure in the triaxial cell is expected to be from atmospheric pressure (0.1 MPa) to a maximum pressure of 20 MPa. The pressure control system includes a pressure/volume controller manufactured by GDS Instruments to control the confining pressure and a high pressure regulator with a Parker needle valve to control the gas pore pressure. Two 32 MPa in-line pore pressure transducers from GDS Instruments were selected to measure the inlet and the outlet gas pressures with an accuracy of 0.15%.

The confining system consists of a 32 MPa pressure/volume controller with a 2×10^{-4} m^3 oil reservoir with a volume accuracy of 0.1%. Volume changes can be measured and displayed to 1×10^{-9} m^3 (0.001 cc). The pressure accuracy is 0.1% of 32 MPa full range output and pressure can be regulated and displayed to 0.008 MPa. In order to provide the hydraulic forces around the sample (confining pressure), the silicone oil 350 (polydimethylsiloxane) supplied by Mistral Lab Chemicals has been used. Silicone oil has been recommended by American Society for Testing and Materials

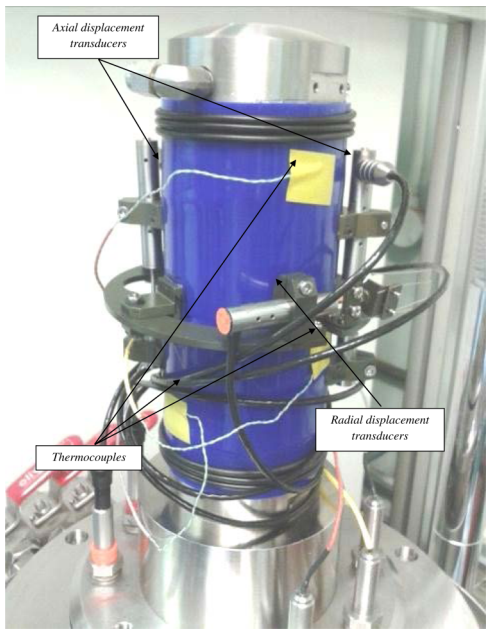

FIG. 5. Displacement transducers and thermocouples attached to the sample in the triaxial cell.

(ASTM) STP-977[32] as the most suitable hydraulic liquid to be used in the triaxial cells. Compared to other cell liquids such as de-aired water, glycerin, castor oil, and liquid paraffin, silicone oil 350 CS does not pass through the rubber sleeve during high pressure tests. It has also shown minimum effects to the rubber sleeve.[31] A liquid suction pump is used to transfer silicone oil from the oil tank to the triaxial cell and vice versa.

An electro-mechanical digital loading frame manufactured by GDS Instruments has also been employed to generate axial load up to 50 kN, applied via a loading ram. The loading system consists of a loading frame and a load cell. The cell base rests on the circular bottom plate and load is applied via movement of the circular plate upward. The loading rate and direction can be controlled using the control box, which has been attached to the loading frame with rates of strain from 1.67×10^{-10} to 1.67×10^{-4} m/s. A 64 MPa internal submersible load cell is placed between the loading shaft and the top of the loading frame including load ram, load button, and electrical connection for data interface with an accuracy of 0.1% of full range output.

2. Temperature control system

Since, the experimental setup has been designed to simulate the *in situ* conditions, it is important that the sample inside the high pressure triaxial cell is kept at a constant temperature corresponding to the *in situ* temperature. In order to control the temperature of the testing sample and providing isothermal conditions, a climate control system has been installed on the high pressure cell. The system comprises four heating elements (Figure 6) and a programmable controller. Heating elements provide constant temperature around the sample from ambient temperature to up to 338 K (65 °C). An aluminium cover with environmental insulation is designated to buffer the cell from changes in atmospheric temperature. The temperature within the sample is measured using three thermocouples attached to the top, middle, and bottom of the sample.

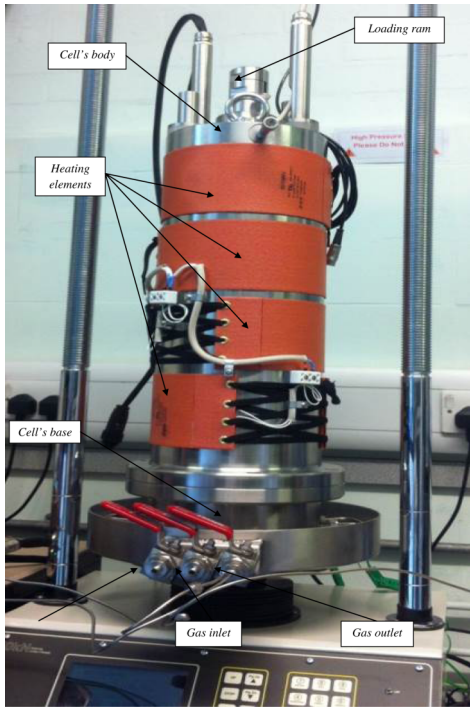

FIG. 6. The high pressure triaxial cell and its components, mounted on the load frame.

Temperature control for other components such as the pipeline, the valves, and the pressure transducers consists of two glass-fibre heating tapes supplied by Bibby Scientific, Ltd. Each heater tape is 2 m long and flexible enough to bend around the pipelines and the connections. A Sensemaster, Ltd, digital three-zone temperature controller has been incorporated with the heater tapes to control the temperature and to provide an isothermal condition for the pipeline.

C. The ancillary system

The ancillary system comprises two main sections including the gas supply unit and gas analysis unit. The gas supply system was designed to deliver different gases with controlled pressure and temperature to both the manometric sorption apparatus and the triaxial core flooding system at pressures up to 30 MPa and temperatures up to 338 K (65 °C). The gas supply system accommodates up to four different pure or mixed gas cylinders. It also includes two sets of pipelines: direct and indirect (Figure 1). The direct line connects the gas cylinders directly to the analysis units if the gas pressure of the cylinder is sufficiently high for the specific experiment. The maximum pressure in this line depends on the maximum pressure of the gas cylinder. The gas pressure can be regulated using high pressure regulators on each cylinder.

The indirect line is used if the gas pressure inside the cylinder is lower than the experimental pressure. The indirect line comprises of Haskel air driven gas booster (model AG-62-50341) to pressurise the gas and a set of gas reservoirs to store the pressurised gases to be used for high gas demand experiments, i.e., high pressure/high flow rate. Syringe pumps are commonly used for pressurising the experimental gases.[33,34,16] In this work, however, adopting a gas booster was preferred due to its lower cost compared to the syringe pump. One limitation of the gas booster is that it has a limited capacity and providing the required volumes of pressurised gas might be time consuming, especially for the experiments with high gas demand. In order to overcome this problem, high pressure vessels are provided as gas reservoirs. For each gas type, two diving cylinders, one in duty and one on standby, are designated. The diving cylinders are rated to a maximum pressure of 30 MPa with an internal volume of 0.012 m^3 (12 l). A regulator adjusts the gas pressure to the desired experimental pressure and conducts the gas from the reservoirs to the experimental units. A pressure relief valve (PRV) is also incorporated into the pipeline with a maximum set pressure of 31 MPa.

A vacuum pump was employed to evacuate the entire system including the dead volumes inside the pipes and the valves to avoid any contamination of injecting gases with the residual gases from previous tests. The ATEX certified Buchi vacuum pump was used with final vacuum of approximately −0.09 MPa. The ATEX certification was necessary since

the flammable gases such as methane are to be used in the system.

In order to investigate the interaction between the sample and various gas species, the composition of outflow gases is determined using an Emerson X-Stream general purpose gas analyser (standard 19 in./3HU version). It comprises two gas channels, one for CO_2 and one for CH_4. Both channels have a defined range of 0%–100%. The gas analyser can be controlled via a web browser interface. The advantage of this analyser is that it is relatively fast and it is capable of analysing the gas samples simultaneously and continuously over a long period of time. Additionally, the calibration procedure is also relatively easy. Prior to each test, the gas analyser is calibrated using N_2 as "zeroing" gas and CO_2 and CH_4 as "span" gases (experimental gases). The manufacturer documents that the optimum gas flow for this gas analyser is 1.7×1^{-5} m^3/s (1 l/min). Therefore, in order to adjust the gas flow, the outflow gas is passed through a low flow rotameter mounted on the wall and equipped with a needle valve to adjust the gas flow. The excess gas is then passed through a one-way valve and eventually is vented to the atmosphere via a fume cupboard.

III. EXPERIMENTAL METHODS AND APPLICATION

A. Sampling and sample preparation

Coal samples of present work were obtained from the Unity coal mine in South Wales, UK (Figure 7). Blocks of coal with dimensions approximately between 0.5 m and 1 m were collected from the 6-ft seam located at an approximate depth of 550 m.

The procedure used for the preparation of powdered samples for the sorption experiments was based on ASTM D-2013[35] including drying, crushing, dividing, and mixing the sample. Following ASTM D-2013[35] and in order to minimise any moisture contamination, air-drying of samples was undertaken. The air-drying stage is important as the presence of excess moisture within the coal sample can influence the coal properties such as sorption capacity, surface area, pore size, density, and porosity.[36,10]

Crushed and ground samples for coal characterisation were passed through a 212 μm sieve.[37,38] For the adsorption and desorption measurements, the crushed samples were size distributed using a series of sieves ranging from 0.5 mm to 2 mm (Figure 8). Size-distributed samples were sealed and labelled separately in air-tight containers and then were stored in a refrigerator to be used in the experiments.

The core samples for the permeability measurements were drilled out from large blocks of coal using a coring machine (Figure 9). A diamond core drill bit with 0.07 m internal diameter was used to drill the core samples. The core samples were then cut into the required lengths using a diamond saw. Special care was taken during the coring and cutting processes to minimise breakage or damage of the coal structure. Any small breakage especially around the edges could potentially damage or puncture the rubber membrane of the sample during triaxial core flooding tests under the high confining pressures and therefore had to be removed. Any sample with major fracture or damaged structure was not used. For broken edges with less than 1 mm width or depth, the ends of the sample were gently filed using a fine sand paper to remove the dents.

In order to prevent breakage of the coal samples under high stress conditions, the ends of the specimens were ground and made parallel to each other using a fine sand paper. This allows a uniform distribution of the axial stresses to both ends of the sample. The core samples were then air-dried for 24 h and wrapped carefully in a plastic cling film. The samples were stored in a refrigerator to be used for the tests.

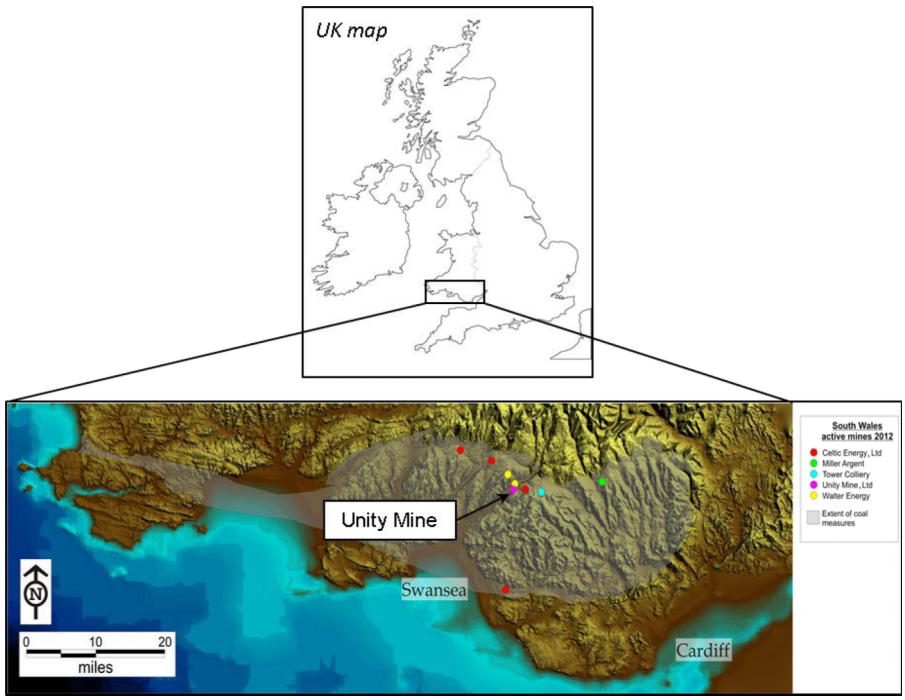

FIG. 7. South Wales coalfield and the locations of the Unity mine and other active mines in the region.

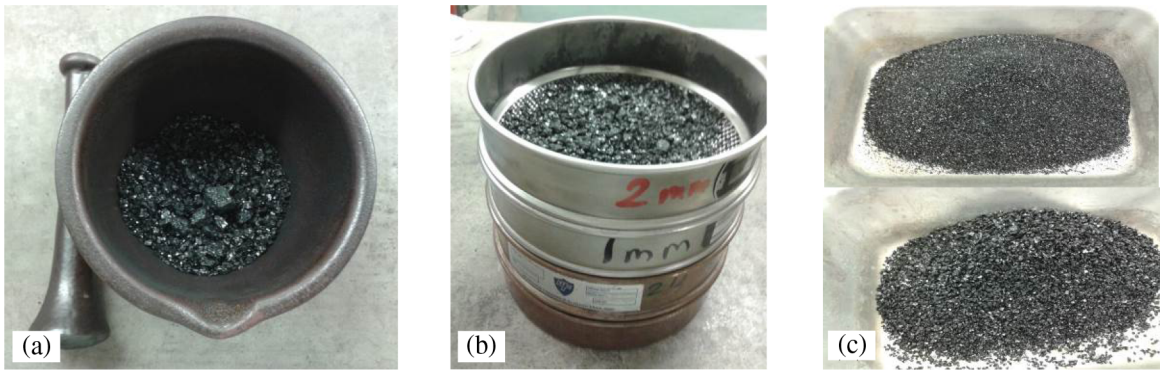

FIG. 8. Sample preparation for adsorption/desorption tests; (a) crushing/grounding, (b) sieving, (c) size-distributed and air-dried samples.

B. Gas adsorption/desorption measurements

Leakage test was conducted prior to each sorption experiment. Helium was injected into the cells at consecutive pressure steps up to 12 MPa. The valves were then shut and the gas pressure in each cell was monitored over 24 h. In order to ensure that no leakage can occur due to the interaction between the O-ring material and gases (in particular for CO_2 experiment), the Viton O-rings were regularly replaced by a new set before conducting each experiment.

The helium expansion or helium pycnometry method has been adopted to determine the void volumes of the reference cell and the sample cell before and after the sample was placed in the sample cell. The advantage of using helium is that the helium gas has the smallest molecule size and can more easily penetrate the small pores than other gases. In addition, helium is a non-reactive gas and therefore, it does not react with the coal inside the sample cell. The void volume in this method can be determined from the measured values of the temperature, pressure, and volume of the injected gas.

The unknown volume of the cell including the dead volumes of the valves and the pipes was determined by injecting a known quantity of helium from a calibration cylinder (pycnometer) into the cell. The pycnometer is a vessel or a container with a precisely known volume (carefully measured by water pycnometry method). A Swagelok stainless steel cylinder has been adopted as a calibration cylinder or pycnometer (Figure 10). The cylinder is a double-ended sample cylinder, pressure rated to 12.4 MPa (1800 psig). It includes a high pressure needle valve and a rupture disc. A heater mat and thermocouple with a temperature controller were used to provide the isothermal conditions during the measurements. The internal volume of the calibration cylinder was measured using water pycnometry.

The helium pycnometry tests comprised three consecutive pressure steps to determine the void volume of the cells, before

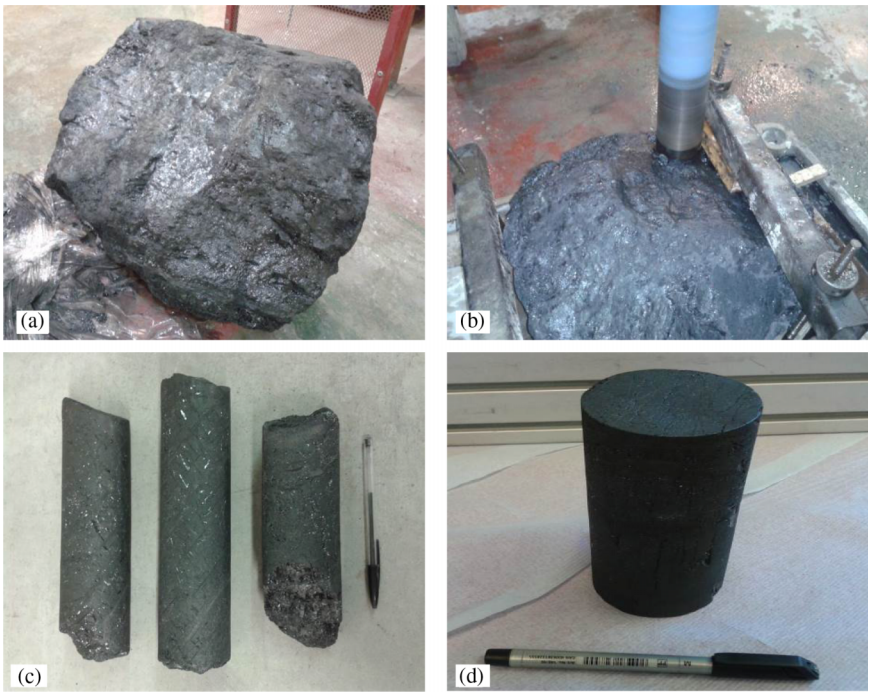

FIG. 9. Sample preparation for the triaxial cell; (a) a large block of coal from the coal mine, (b) a coring machine with a 70 mm diamond core drill bit, (c) the coal samples after the coring, (d) the coal sample after cutting the ends and polishing.

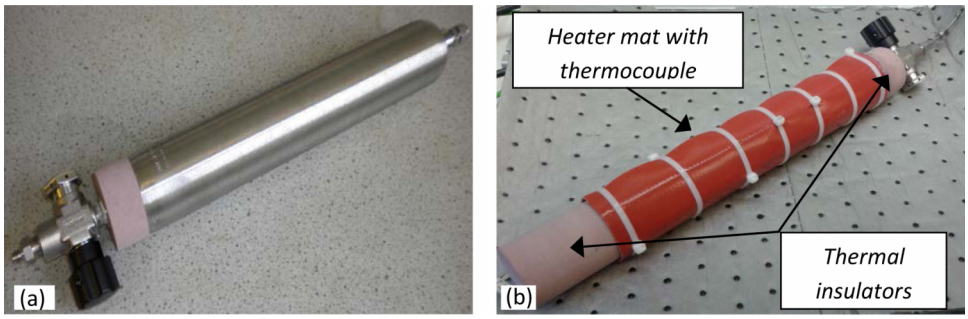

FIG. 10. (a) Volume calibration cylinder, (b) calibration cylinder after attaching the heater mat, thermocouple, and thermal insulators.

and after sample loading.[21] The compressibility factor of helium was calculated based on gas pressure and temperature using the relationship provided by Sudibandriyo.[39]

Determining the void volume was carefully carried out as small errors can have a considerable impact on the mass balance calculation.[25] In order to minimise the errors, void volume measurements were performed in multiple series of helium pycnometeries at successive gas injection pressures from 1.2 MPa to 2.1 MPa.

In order to investigate the effect of the initial gas injection pressures on the accuracy of the measured void volume, a number of helium pycnometeries were also performed at several initial injection pressures. The results of the volumes estimated for both the reference cell and the sample cell are presented in Figure 11. At low pressures, the margin of the errors was much larger, i.e., the range of measured volume including the dead volume varied between 250 and 400 cm^3. As the initial pressure was increased, the estimated values for both reference cell and sample cell showed more convergence and the differences in measurements became less than 20 cm.[3] Therefore, improved accuracy was achieved with increasing the initial injection pressures to more than 1 MPa. In addition, the pressure transducers used have a broad range of pressure (20 MPa), and their accuracy improves at higher pressures. Therefore, all measurements were performed at initial gas injection pressures higher than 1 MPa.

In order to evaluate the precision of the volume measurements with the calibration cylinder, data from several volume measurements for an empty reference cell were analysed.

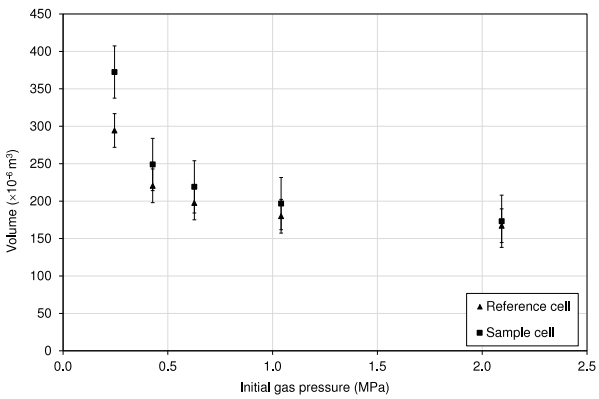

FIG. 11. The results of the helium pycnometry performed at several initial gas pressures.

The initial gas pressures in these measurements were ranging between 2 and 4.5 MPa. After analysing the results, an error margin of ±0.79% was found which is within the acceptable range. Similar analysis was also performed for the empty and loaded sample cell. Similar to the reference cell, the error margin for the empty sample cell was estimated to be small, i.e., less than ±0.8%. However, for the loaded sample cell the margin of error was slightly larger (±1%). This can be attributed to mechanical compression or expansion of the sample during the gas injection/extraction process.[26] In addition, a small fraction of fine particles of the sample could have been lost during the gas extraction and vacuum processes. The latter issue however was minimised by placing filter papers at the inlet and outlet of the sample cell.

50 g of powdered coal sample was carefully weighed to the nearest mg and placed inside the sample cell. Filter papers (2 μm) were used to prevent coal particles entering the valves and pipes during the experiment. The adsorption cell loaded with the sample was placed inside the water bath and the temperature was set to 298 K. Several hours were allowed for the thermal equilibration and then the measurements were carried out.

Figure 12 shows a schematic diagram of the step by step experimental procedure adopted for manometric measurements. Prior to each test, a vacuum pump was used to evacuate the entire system including the pipes, valves, and cells to avoid potential contaminations of injecting gas with the remaining gases from previous tests. The volumes of the reference cell and the sample cell were measured before and after placing the sample in the sample cell using the helium pycnometry method as described in Sec. III B.

C. Gas permeability measurements

The experimental procedure used for gas transport studies including assembling the core sample in the triaxial cell and preparing the triaxial cell and related components is described step by step. In addition, the methodology that has been employed to measure the gas flow and permeability of the coal samples to different gases is described in detail.

After initial measurements (dimensions and weight), the core sample was wrapped with a thick polytetrafluoroethylene (PTFE) tape before placing in a silicon rubber sleeve (Figure 13(a)). The PTFE tape was used to protect the rubber sleeve from any sharp edges that have remained on the coal surface.

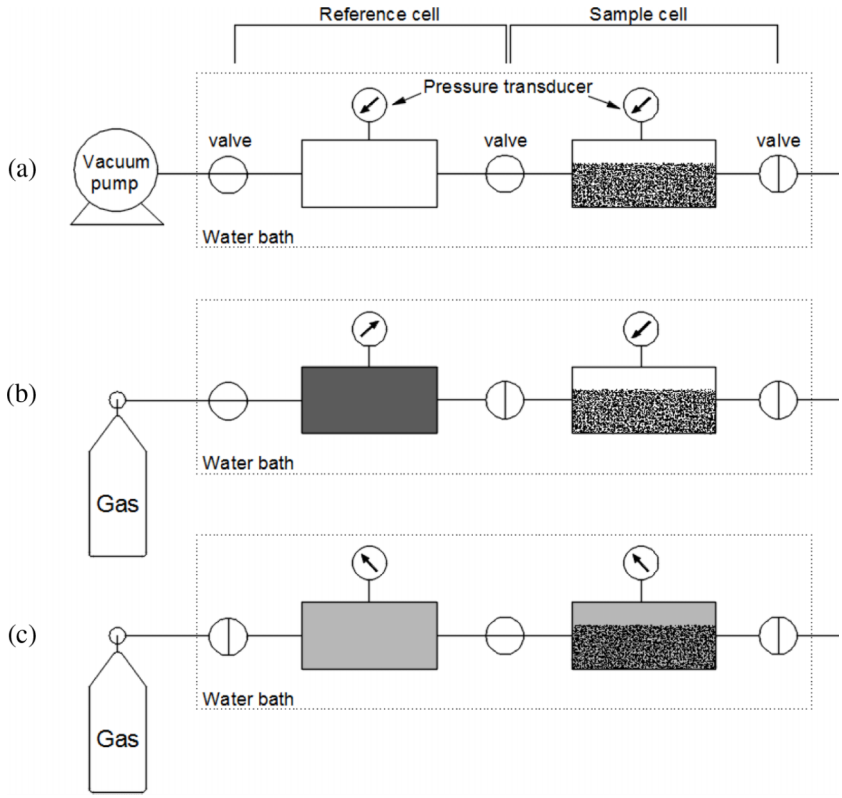

FIG. 12. Schematic diagram of the manometric method, (a) prior to each test, the system is evacuated by a vacuum pump, (b) gas is injected into the reference cell with required pressure, and (c) the cells are connected by opening the middle valve. Steps (b) and (c) are repeated until the final pressure level was achieved.

A 1.5 mm thick blue silicone rubber has been used as a membrane (Figure 13(b)). In comparison with other materials such as latex and nitrile, silicone rubber proved to be a stronger material against puncturing and less reactive with chemicals especially with CO_2 gas. O-rings were used to secure both ends of the membrane to the base and top of the cell and to prevent gas leakage into the silicone oil or vice versa.

The displacement transducers, two axial and one radial, were then attached to the sample (Figure 5). The three thermocouples were also attached to the top, middle, and bottom of the sample to record the temperature variations across the sample during the test.

The top cap was then placed and the cell was filled with the silicone oil using a manual oil pump. The inlet and outlet pipes were connected as well as the pressure transducers and the mass flow meters. Prior to each test, both pressure transducers and flow meters were calibrated by manually setting them to zero at atmospheric pressure condition. The temperature of the system was set to a desired value and kept constant throughout the test. A certain amount of confining pressure, i.e., 1 MPa

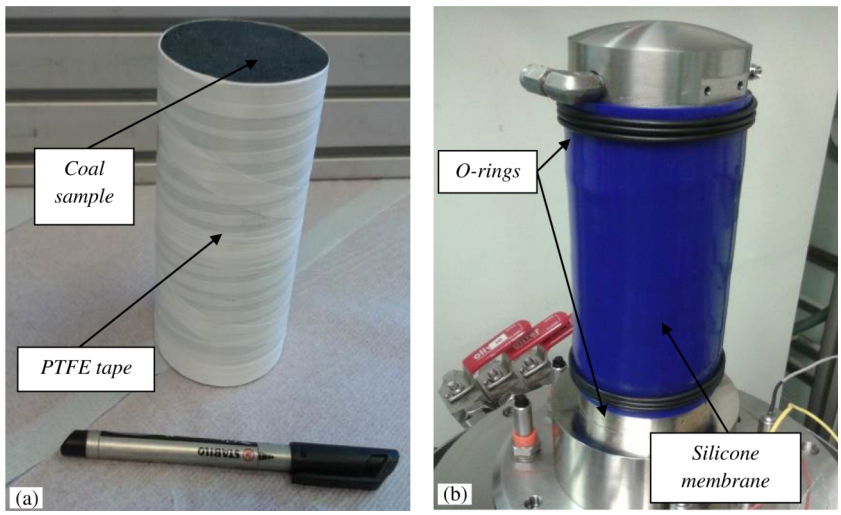

FIG. 13. Preparation of the core samples for the triaxial cell. (a) Sample is wrapped with the PTFE tape, (b) sample is placed in a silicone rubber membrane and secured to the top and the bottom of the cell using the O-rings.

was applied to avoid oil leakage into the sample during the vacuum process. A small amount of vacuum (approximately −0.03 to −0.05 MPa) was applied at downstream of the sample while upstream valve was closed. Depending on the sample conditions, the vacuum process can take few hours to more than a day. After vacuuming the sample, downstream valve was closed and experimental gas was injected at the upstream. The applied gas pressure at this stage was very low, i.e., 0.2 MPa and was increased slowly. It was important that sudden increases of gas pressure or confining pressures are avoided to prevent gas or oil leakage as well as failure of the membrane or sample. The upstream pressure was increased step by step to the maximum experimental pressure and was kept constant until the sample was completely saturated. Depending on the test conditions and gas type, saturation of the sample can be achieved within few hours or few days. In the present study, in most cases, saturation was achieved within 3–6 days. The condition for achieving the saturation state was based on pressure decrease less than 0.05 MPa over 24 h as suggested by van Hemert *et al.*[18]

The steady-state method was used to estimate the permeability of the coal samples to various gases. The confining pressure was maintained at the desired pressure and increased step by step. The gas pressure at the upstream end was fixed at a range of pressures. The downstream pressure was constantly kept at atmospheric pressure (0.1 MPa). Once the steady-state flow rate was achieved, gas pressure at the upstream end was increased to the next level. Figure 14 presents an example of the experimental measurements during gas flow rate measurements using helium on a coal sample. The effective stresses were calculated as the difference of the confining pressure and the mean pore gas pressure. The mean pore gas pressures were estimated as the average gas pressures at upstream and downstream of the sample.

IV. GAS ADSORPTION BEHAVIOUR IN COAL

In order to determine the gas adsorption isotherm, the gas was admitted to the reference cell at a desired pressure. The reference cell was then connected to the sample cell. At this stage, the gas pressure decreases depending on the void volume (V_v). Immediately after admitting the gas to the sample cell, a sudden fluctuation in gas pressure and temperature is observed which decays gradually after a short time. This is attributed to the adiabatic (Joules-Thomson) cooling of injected gas.[40,41] The pressure decrease may continue for several hours to several days, depending on gas specie, sample size, and kinetics of process, until the system reaches the equilibrium condition. The above steps were repeated until the final pressure level was achieved.

The initial amount of the gas injected in the reference cell and the amount of the unadsorbed (free) gas were calculated based on the pressure, temperature, and volume of the cells, using the ideal gas law.[27] The compressibility factors for CO_2, CH_4, and N_2 gases were calculated based on PR-EoS proposed by Peng and Robinson.[28] The excess adsorption $\left(n_{ads}^{ex}\right)$ was then calculated directly from the experimental measurements, using the mass balance between the reference cell and the sample cell at each step of gas injection,[27]

$$n_{ads}^{ex} = \frac{1}{RT}\left[\frac{P_{ref}V_{ref}}{Z_{ref}} - \frac{P_{eq}\left(V_{ref}+V_v\right)}{Z_{eq}}\right], \tag{3}$$

where P_{ref} is the gas pressure in the reference cell (Pa), V_{ref} is the volume of the reference cell (m^3), Z_{ref} is the compressibility factor, R is the universal gas constant (J/mol K), and T is the temperature (K). P_{eq} is the pressure of free gas at equilibrium (Pa), Z_{eq} is the compressibility factor of the free gas. Details of derivation of Equation (3) can be found in the work of Mosleh[29] and Condon.[27]

The cumulative quantity of gas introduced through the reference cell into the sample cell was evaluated by summing up the quantities introduced in each pressure step. Gensterblum *et al.*[25] recommended a maximum of 20 pressure steps in the manometric method due to the errors for each pressure step that have an incremental effect on error development in the final step.

Figure 15 presents the results of total excess adsorption isotherms versus gas equilibrium pressure for N_2, CH_4, and CO_2 gases at 298 K. Figure 15 shows that the amount of N_2 excess adsorption gradually increases with the increase in gas pressure and reached to a maximum value of 0.85 mol/kg at an equilibrium pressure of 11 MPa. In the case of CH_4, the excess adsorption increased with the increase in gas pressure and

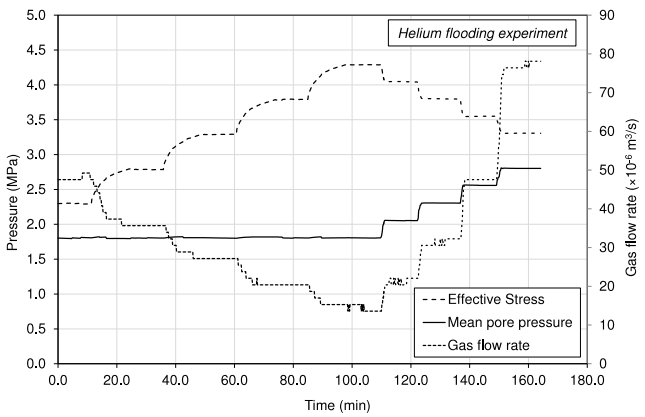

FIG. 14. Variations of gas flow rates during helium flooding experiment (at 298 K).

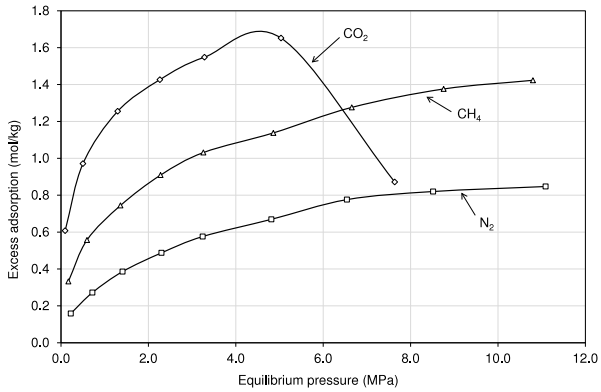

FIG. 15. Excess adsorbed amounts of N_2, CH_4, and CO_2 gases on an anthracite coal sample from South Wales coalfield.

reached to a maximum value of 1.4 mol/kg at an equilibrium pressure of 11 MPa. For the case of CO_2, however, different adsorption behaviour was observed. The excess adsorption gradually increased and reached to a maximum value of 1.7 MPa at approximately 4.5 MPa, followed by a sharp decrease.

The decrease in the excess adsorption of CO_2 has been related to the volumetric effects that can occur during CO_2 adsorption/desorption processes.[8] The volumetric effects have collectively increased the sample volume and reduced the void volume of the cell during the experiment. This effect becomes more visible when the volume increase can no longer be compensated by the gas uptake in the coal porous structure.

V. GAS FLOW AND PERMEABILITY EVOLUTION IN COAL

During core flooding experiments, the gas flow behaviour and permeability evolution of the coal samples were investigated for a range of gas injection pressures and confining pressures. At each steady-state condition, the gas flow rate was recorded and permeability of the coal sample was calculated using Darcy's law (Equation (2)).

Figure 16 presents the results of the helium flow rates versus differential pressures obtained for a range of gas injection pressures up to 5.5 MPa and confining pressures up to 6 MPa at 298 K. Despite a certain pressure gradient across the sample, no flow could be recorded at low pressures within the time scale allowed, i.e., 15–30 min. This effect has been attributed to "threshold phenomenon."[42] Accordingly, a certain non-zero pressure gradient (1.7 MPa/m) was required to initiate the flow. The overall gas flow rate was increased with increases in the gas injection pressure. A maximum value of 88×10^{-6} m^3/s at approximately 5.5 MPa differential gas pressure and 6 MPa confining pressure has been observed. In addition, under constant gas injection pressures, a considerable decrease in the gas flow rate was observed as a result of increases in the confining pressure applied.

The results presented in Figure 16 exhibited a slight non-linearity between the volumetric gas flow rate and the differential pressure across the sample for the injection test with helium, especially at lower confining pressures (3 MPa and less). According to Darcy's law, the relationship between gas flow rate and differential pressure is considered to be linear. Due to non-reactivity of helium in coal, the effect of sorption on the flow behaviour was considered to be negligible. In addition, due to relatively short duration for each permeability measurement test (less than 30 min), the influence of gas diffusion into the coal matrix on gas flow rates was considered to be insignificant. Therefore, it was assumed that the observations mainly reflect the flow behaviour in the cleat system.

The non-linearity observed between the gas flow rate and differential pressure has also been reported by other researchers. Jasinge *et al.*[43] have mentioned the possibility of a transition of the flow regime to a non-Darcian gas flow. The non-linearity in gas flow behaviour has been also attributed to the influence of changes in the effective stress on cleat permeability[22,43–45] and strong dependency of cleat volume compressibility to mean pore pressure, especially at low pressures.[17] In addition, the compliance of the system due to changes in stress conditions can also be influential on the non-linearity observed between the gas flow rates and differential gas pressure.

The linearity of the flow, however, has improved at higher pressures. This could be due to the fact that under higher confining pressures, potential changes in the stress regime have less effect on pore morphology.[43] In other words, at higher confining stresses, the changes in cleat volume compressibility are reduced providing less sensitivity of the flow rate to the effective stress.[17,22]

Figure 17 presents the absolute permeability of the coal sample at different gas pressures and confining pressures. At a constant confining pressure of 1 MPa, the absolute permeability of the coal sample was increased considerably by the increase in gas injection pressure and reached to a maximum value of 1.35×10^{-15} m^2 (at differential gas pressure of 0.6 MPa). The gas injection pressure was then kept constant and the confining pressure was increased to 2 MPa. As a result, the coal permeability decreased by 68%. After considerable changes observed in the first stage, the

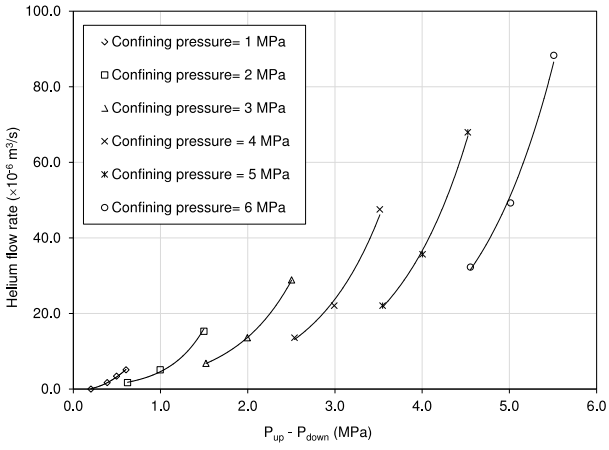

FIG. 16. Helium flow rates versus differential gas pressure between the upstream and downstream at various confining pressures (T = 298 K).

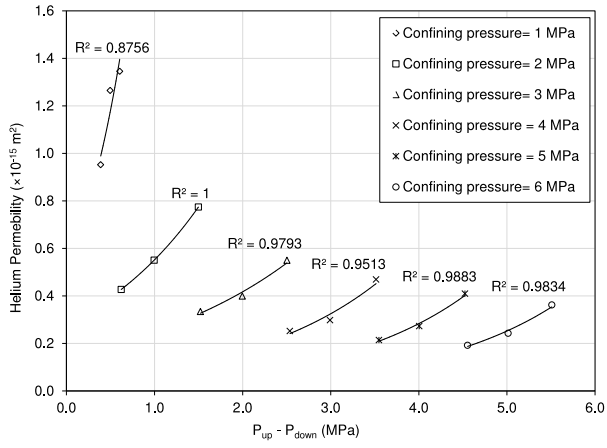

FIG. 17. Absolute permeability of the coal sample to helium versus differential gas pressure between upstream and downstream at various confining pressures (T = 298 K).

permeability variations due to increase in gas pressure or confining pressure became steadier. At constant gas injection pressures, an average permeability reduction of 54% was observed for every 1 MPa increase in confining pressure. The lowest absolute permeability, i.e., 0.19×10^{-15} m^2, was obtained at the confining pressure of 6 MPa and differential gas pressure of 4.5 MPa. Overall, an average permeability reduction of 78% was estimated during the course of this experiment.

VI. CONCLUSIONS

An experimental facility has been developed to investigate the sorption behaviour and reactive transport of gases in coal under high pressure conditions. The facility comprises (i) a manometric sorption apparatus, (ii) a triaxial core flooding system, and (iii) the ancillary system including the gas supply unit and gas analysis unit. The manometric sorption apparatus is capable of measuring adsorption/desorption isotherms of various gas species on powdered and intact samples at gas injection pressures up to 20 MPa and temperatures up to 338 K. The triaxial core flooding system is capable of replicating the *in situ* conditions in terms of pore pressure and confining pressure for depths up to 2000 m. Using the bespoke triaxial core flooding system, the gas flow behaviour, the permeability of the sample to various gas species, and sorption-induced swelling/shrinkage of the sample can be studied under a broad range of effective stress conditions, i.e., gas pore pressures and confining pressures up to 20 MPa.

The broad range of sample sizes (from powdered sample to large intact core samples with up to 0.7 m diameter) that can be accommodated within the apparatus and the broad range of gas pressures (up to 20 MPa) that can be applied provide an advanced experimental platform to expand the knowledge of gas transport and reactions in coal. The features of the facilities developed enable a simultaneous run of the experiments using both units, i.e., the gas sorption apparatus and the triaxial core flooding system. This is considered to be an important advantage due to the long-term nature of the experiments. A high level of accuracy and resolution of the dataset has been obtained and presented in this paper by designing and adopting appropriate measuring/monitoring devices.

A comprehensive set of data, including gas sorption and transport properties of the anthracite coal samples from South Wales coalfield, has been produced which is believed to be for the first time. The results of the excess sorption of CO_2 in powdered coal samples have shown a considerable volumetric effect which is related to the swelling effect of CO_2 on coal matrix. The results of core flooding experiments with helium showed strong dependency of the coal permeability to changes in pore pressure and effective stress, especially at lower pressures.

ACKNOWLEDGMENTS

The financial support received from the Welsh-European Funding Office as part of the Geoenvironmental Research Centre's SEREN project is gratefully acknowledged. The authors would like to thank Dr. Snehasis Tripathy for his support. We also thank GDS Instruments for their contribution in the construction and commissioning of the laboratory equipment described. Technical support from the technicians and staff of the Engineering Workshop at Cardiff University is gratefully acknowledged.

[1]E. Hendriks, G. M. Kontogeorgis, R. Dohrn, J.-C. de Hemptinne, I. G. Economou, L. F. Žilnik, and V. Vesovic, "Industrial requirements for thermodynamics and transport properties," Ind. Eng. Chem. Res. **49**, 11131–11141 (2010).

[2]E. Ozdemir, K. Schroeder, and B. I. Morsi, "Global warming: Carbon dioxide sequestration in coal seams," Proc. Am. Chem. Soc. **42**, 310–317 (2002), available at https://scholar.google.co.uk/citations?view_op=view_citation&hl=en&user=LlJm88wAAAAJ&citation_for_view=LlJm88wAAAAJ:Y0pCki6q_DkC.

[3]C. M. White, D. H. Smith, K. L. Jones, A. L. Goodman, S. A. Jikich, R. B. LaCount, S. B. DuBose, E. Ozdemir, B. I. Morsi, and K. T. Schroeder, "Sequestration of carbon dioxide in coal with enhanced coalbed methane recovery—A review," Energy Fuel **19**(3), 659–724 (2005).

[4]T. Fujii, Y. Sato, H. Lin, H. Inomata, and T. Hashida, "Evaluation of CO_2 sorption capacity of rocks using a gravimetric method for CO_2 geological sequestration," Energy Procedia **1**(1), 3723–3730 (2009).

[5]S. Day, R. Fry, and R. Sakurovs, "Swelling of Australian coals in supercritical CO_2," Int. J. Coal Geol. **74**(1), 41–52 (2008).

[6]S. Ottiger, R. Pini, G. Storti, and M. Mazzotti, "Competitive adsorption equilibria of CO_2 and CH_4 on a dry coal," Adsorption **14**(4-5), 539–556 (2008).

[7]J. E. Fitzgerald, Z. Pan, M. Sudibandriyo, J. R. L. Robinson, K. A. M. Gasem, and S. Reeves, "Adsorption of methane, nitrogen, carbon dioxide and their mixtures on wet Tiffany coal," Fuel **84**(18), 2351–2363 (2005).

[8]N. Siemons and A. Busch, "Measurement and interpretation of supercritical CO_2 sorption on various coals," Int. J. Coal Geol. **69**(4), 229–242 (2007).

[9]P. van Hemert, H. Bruining, E. S. J. Rudolph, K. A. A. Wlof, and J. G. Mass, "Improved manometric setup for the accurate determination of supercritical carbon dioxide sorption," Rev. Sci. Instrum. **80**(3), 035103 (2009).

[10]E. Ozdemir, "Chemistry of the adsorption of carbondioxide by Argonne Premium coals and a model to simulate CO_2 sequestration in coal seams," Ph.D. thesis, University of Pittsburgh, 2004.

[11]F. M. Nelsen and F. T. Eggertsen, "Improvements in or relating to method and apparatus for the estimation of surface areas of solids," British patent 831639 (30 April 1958).

[12]S. Sircar, "Gibbsian surface excess for gas adsorptions revisited," Ind. Eng. Chem. Res. **38**(10), 3670–3682 (1999).

[13]N. Wakao, S. Kaguei, and J. M. Smith, "Adsorption chromatography measurements. Parameter determination," Ind. Eng. Chem. Fundam. **19**(4), 363–367 (1980).

[14]P. Massarotto, S. D. Golding, J. S. Bae, R. Iyer, and V. Rudolph, "Changes in reservoir properties from injection of supercritical CO_2 into coal seams—A laboratory study," Int. J. Coal Geol. **82**(3-4), 269–279 (2010).

[15]G. G. X. Wang, X. Zhang, X. Wei, X. Fu, B. Jiang, and Y. Qin, "A review on transport of coal seam gas and its impact on coalbed methane recovery," Front. Chem. Sci. Eng. **5**(2), 139–161 (2011).

[16]S. Mazumder, A. Karnik, and K. H. Wolf, "Swelling of coal in response to CO_2 sequestration for ECBM and its effect on fracture permeability," SPE J. **11**(3), 390–398 (2006).

[17]Y. Gensterblum, A. Ghanizadeh, and B. M. Krooss, "Gas permeability measurements on Australian subbituminous coals: Fluid dynamic and poroelastic aspects," J. Nat. Gas Sci. Eng. **19**, 202–214 (2014).

[18]P. van Hemert, K. A. A. Wolf, and E. S. J. Rudolph, "Output gas stream composition from methane saturated coal during injection of nitrogen, carbon dioxide, a nitrogen-carbon dioxide mixture and a hydrogen-carbon dioxide mixture," Int. J. Coal Geol. **89**, 108–113 (2012).

[19]S. Durucan, M. Ahsan, and J. Q. Shi, "Matrix shrinkage and swelling characteristics of European coals," Energy Procedia **1**(1), 3055–3062 (2009).

[20]S. Harpalani and A. Mitra, "Impact of CO_2 injection on flow behavior of coalbed methane reservoirs," Transp. Porous Media **82**(1), 141–156 (2010).

[21]Z. Pan, L. D. Connell, and M. Camilleri, "Laboratory characterisation of coal reservoir permeability for primary and enhanced coalbed methane recovery," Int. J. Coal Geol. **82**(3-4), 252–261 (2010).

[22]Z. Chen, Z. J. Pan, J. S. Liu, L. D. Connell, and D. Elsworth, "Effect of the effective stress coefficient and sorption-induced strain on the evolution

of coal permeability: Experimental observations," Int. J. Greenhouse Gas Control **5**(5), 1284–1293 (2011).
[23]P. G. Ranjith and M. S. A. Perera, "A new triaxial apparatus to study the mechanical and fluid flow aspects of carbon dioxide sequestration in geological formations," Fuel **90**(8), 2751–2759 (2011).
[24]P. Carles, P. Egermann, R. Lenormand, and J. Lombard, "Low permeability measurements using steady-state and transient methods," in The International Symposium of the Society of Core Analysts, Calgary, Canada, 10–14 September 2007.
[25]Y. Gensterblum, P. van Hemert, P. Billemont, E. Battistutta, A. Busch, B. M. Krooss, G. De Weireld, and K. H. A. A. Wolf, "European inter-laboratory comparison of high pressure CO_2 sorption isotherms II: Natural coals," Int. J. Coal Geol. **84**(2), 115–124 (2010).
[26]S. Mohammad, J. E. Fitzgerald, J. R. L. Robinson, and K. A. M. Gasem, "Experimental uncertainties in volumetric methods for measuring equilibrium adsorption," Energy Fuel **23**(1), 2810–2820 (2009).
[27]J. B. Condon, *Surface Area and Porosity Determinations by Physisorption, Measurements and Theory* (Elsevier, Amsterdam, 2006).
[28]D. Y. Peng and D. B. Robinson, "A new two-constant equation of state," Ind. Eng. Chem. Fundam. **15**(1), 59–64 (1976).
[29]M. Hadi Mosle, "An experimental investigation of flow and reaction processes during gas storage and displacement in coal," Ph.D. thesis, Cardiff University, 2014.
[30]P. C. Carman, *Flow of Gases Through Porous Media* (Butterworths, London, 1956).
[31]A. J. Smits and J. P. Dussauge, *Turbulent Shear Layers in Supersonic Flow*, 2nd ed. (American Institute of Physics, New York, 2006).
[32]ASTM Standards, in *ASTM STP-977Advanced Triaxial Testing of Soil and Rock*, edited by R. T. Donaghe, R. C. Chaney, and M. L. Silver (ASTM International, West Conshohocken, PA, 1988).
[33]S. Hol, C. J. Peach, and C. J. Spiers, "Applied stress reduces the CO_2 sorption capacity of coal," Int. J. Coal Geol. **85**(1), 128–142 (2011).
[34]E. Ozdemir and K. Schroeder, "Effect of moisture on adsorption isotherms and adsorption capacities of CO_2 on coals," Energy Fuels **23**(1), 2821–2831 (2009).
[35]ASTM Standards, *ASTM D-2013, Standard Practice of Preparing Coal Samples for Analysis* (ASTM International, West Conshohocken, PA, 2012), Vols. 05 and 06.
[36]J. G. Speight, *Handbook of Coal Analysis* (John Wiley & Sons, Inc., Hoboken, New Jersey, 2005).
[37]ASTM Standards, *ASTM D-5142, Standard Test Methods for Proximate Analysis of the Analysis Sample of Coal and Coke by Instrumental Procedures* (ASTM International, West Conshohocken, PA, 2009), Vols. 05 and 06.
[38]ASTM Standards, *ASTM D-5373, Standard Test Methods for Instrumental Determination of Carbon, Hydrogen, and Nitrogen in Laboratory Samples of Coal* (ASTM International, West Conshohocken, PA, 2013), Vols. 05 and 06.
[39]M. Sudibandriyo, "Measurement of methane, nitrogen and carbon dioxide adsorption on wet selected coals," in *Proceedings of Seminar Nasional Teknologi Proses Kimia VI* (Jakarta, 2004), pp. 1–9.
[40]W. S. Han, K.-Y. Kim, M. Lu, B. J. McPherson, C. Lu, and S.-Y. Lee, "Injectivity changes and associated temperature disequilibrium: Numerical study," Energy Procedia **4**, 4552–4558 (2011).
[41]M. S. Gruszkiewicz, M. T. Naney, J. G. Blencoe, D. R. Cole, J. C. Pashin, and R. E. Carroll, "Adsorption kinetics of CO_2, CH_4 and their equimolar mixture on coal from the Black Warrior Basin, West-Central Alabama," Int. J. Coal Geol. **77**(1-2), 23–33 (2009).
[42]Z. Chen, G. Huan, and Y. Ma, *Computational Methods for Multiphase Flows in Porous Media (Computational Science and Engineering)* (Society for Industrial and Applied Mathematics (SIAM), Philadelphia, 2006).
[43]D. Jasinge, P. G. Ranjith, and S. K. Choi, "Effects of effective stress changes on permeability of latrobe valley brown coal," Fuel **90**(3), 1292–1300 (2011).
[44]V. Vishal, P. G. Ranjith, and T. N. Singh, "CO_2 permeability of Indian bituminous coals: Implications for carbon sequestration," Int. J. Coal Geol. **105**, 36–47 (2013).
[45]M. S. A. Perera, P. G. Ranjith, S. K. Choi, and D. Airey, "The effects of sub-critical and super-critical carbon dioxide adsorption-induced coal matrix swelling on the permeability of naturally fractured black coal," Energy **36**(11), 6442–6450 (2011).